Carbohydrate Polymers 84 (2011) 686–689

Contents lists available at ScienceDirect

Carbohydrate Polymers

journal homepage: www.elsevier.com/locate/carbpol

Short communication

Self-assembled liquid crystal film from mechanically defibrillated chitosan nanofibers

Dagang Liu[a,b,*], Qinglin Wu[b], Peter R. Chang[c,**], Guizhi Gao[a]

[a] Jiangsu Provincial Key Laboratory of Atmospheric Environment Monitoring and Pollution Control, School of Chemistry, Nanjing University of Information Science & Technology, Nanjing, Jiangsu 210044, China
[b] School of Renewable Natural Resources, Louisiana State University Agricultural Center, Baton Rouge, LA 70803, USA
[c] Bioproducts and Bioprocesses National Science Program, Agriculture and Agri-Food Canada, Saskatoon, SK, S7N 0X2 Canada

ARTICLE INFO

Article history:
Received 9 October 2010
Received in revised form
24 November 2010
Accepted 8 December 2010
Available online 16 December 2010

Keywords:
Chitosan
Nanofiber
Liquid crystal

ABSTRACT

Wet-grinding and high-pressure homogenization were combined to defibrillate chitosan particles into nanoscaled fibrils, and the obtained nanofiber was made into a high strength liquid crystal film by self-organization at relatively low temperature. Mechanically disassembled chitosan nanofibers showed an average diameter of 50 nm. The fabricated transparent liquid crystal film had a high tensile strength of 100.5 ± 4.0 MPa and a Young's modulus of 2.2 ± 0.2 GPa due to its ordered, layered, and porous-free structure. A green, efficient and reliable approach for producing chitosan nanofibers and liquid crystal film has been developed.

© 2010 Elsevier Ltd. All rights reserved.

1. Introduction

Many biomacromolecules in biological tissues are known to self-assemble from nanofibrils into an ordered hierarchy with a liquid crystalline (LC) phase structure, e.g. the exoskeleton of arthropods is composed of chitin and glycoprotein (Bouligand, 1978, 2008), which are covalently linked together. The typical size of a chitin crystallite is approximately 3 nm in diameter and consists of 19 hydrogen-bonded molecular chains. The macromolecular chitin chains line up in parallel to form a microfibril; a bundle of such microfibrils then forms a sheet followed by formation of helicoidal stack layer. Each layer of crystallites changes orientations through a small angle from layer to layer in a constant direction of rotation to form a uniaxial nematic LC structure in a helical fashion (Belamie, Mosser, Gobeaux, & Giraud-Guille, 2006). A chiral nematic LC phase has also been found in rod-like cellulose suspension and its solidified films (Lima & Borsali, 2004; Roman & Gray, 2005). Jung reported the LC thermodynamic phase behavior of amyloid protein fibers in water and discussed at length the effect of the source of protein fibers on the colloidal nematic phase transition (Jung & Mezzenga, 2010). It is worth noting that biological liquid crystals perform excellent mechanical functions; for example, spider silk has been found to exhibit excellent mechanical properties, such as high yield stress comparable to that of high-tensile steel (Vollrath & Knight, 2001). Biomimetic biological liquid crystal materials self-assembled from micro or nano-fibrils have been anticipated to be widely used as biomaterials, biosensors, pharmaceutical carriers, and so on (Kato, 2002). Until now, no chitosan was ever reported as LCs because of its limited solubility in aqueous acids but its derivatives did (Rout, Barman, Pulapura, & Gross, 1994). Although electrospinning from several poisonous organic solvents is a method of fabrication of pure chitosan (CS) or blended chitosan nanofibers, results show that the thread-like spun nanofibers are amorphous, unstable in aqueous solution, and have poor mechanical properties (Gong et al., 2008).

In this communication we report a simple, versatile, mechanical top-down approach to disassembling uniform chitosan nanofibrils in an aqueous system using a combination of wet milling and microfluidic homogenization. The high strength LC film was then reassembled bottom-up from chitosan nanofibrous colloidal suspension. The mechanical and optical properties of the LC film were also investigated. We hope to provide green, reliable, and efficient methods for preparing chitosan nanofiber and high-strength nanofibril LC material.

2. Experimental

Chitosan with a degree of deacetylation of 90% and a Mw of 161 kDa was provided by the Vanson HaloSource Company

* Corresponding author at: Jiangsu Provincial Key Laboratory of Atmospheric Environment Monitoring and Pollution Control, School of Chemistry, Nanjing University of Information Science & Technology, Nanjing, Jiangsu 210044, China.
** Corresponding author.
E-mail addresses: dagangliu@gmail.com (D. Liu), peter.chang@agr.gc.ca (P.R. Chang).

0144-8617/$ – see front matter © 2010 Elsevier Ltd. All rights reserved.
doi:10.1016/j.carbpol.2010.12.028

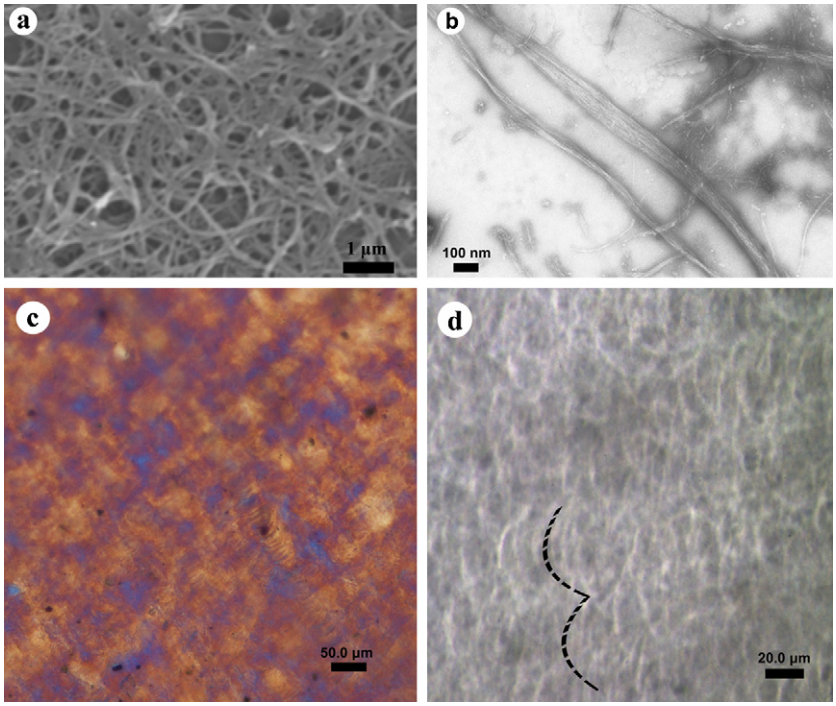

Fig. 1. SEM (a), TEM (b) micrographs of chitosan nanofibrils, and POM micrographs of chitosan LC film (c and d).

(Seattle, WA). A target amount of raw chitosan powder was poured into distilled water to obtain a slurry with 0.1 wt% dry sample weight. After 5 min of stirring, the slurry was poured into a wet-grinding machine (Labor-pilot 2000/4, IKA® Works, Inc.) with a milling gap of about 0.2 mm. The chitosan slurry was forced to pass through the gap with a flow speed of 10 L/h for 5 cycles to produce a milling slurry. The milling sample was then poured into the stainless-steel holding tank of a Microfluidizer (M-100P, Microfluidics Corp. MA, USA), which was equipped with a pair of ceramic (200 μm) and diamond (87 μm) interaction chambers. The slurry was cooled by passing through a stainless coil submerged in an ice bath, and then released back to the tank for the next treatment cycle. Under a constant pressure of 207 MPa, the ground slurry passed through the interaction chambers at a rate of 133 mL/min for 10 passes. The obtained homogenized chitosan slurry was subsequently centrifuged at 1000 rpm for 5 min (Sorvall RC-5B Refrigerated Superspeed Centrifuge, Du Pont Instruments) to remove the sediment and produce a homogeneous chitosan suspension (which is noted as CS suspension). The suspension was poured into a glass Petri dish and then placed in a refrigerator at 10 °C for slow water-evaporation to fabricate an LC thin film with a thickness of 0.5 mm. As a contrast, a cast film was prepared by evaporating water from the suspension in an aluminum dish at 40 °C.

Scanning electron microscopy (SEM) was performed using a Hitachi S-3600N VP SEM (Hitachi, Japan) to investigate the morphology of the chitosan nanofibers and its LC film. Chitosan nanofibrous suspension was spread out on copper grids coated with carbon support film and then coated with gold for observation at 20 kV. The surface and cross-section of the LC film were also coated with gold for SEM analysis. Transmission electron microscopy (TEM) observations were carried out on a JEOL JEM 2010 FEF (UHR) electron microscope with an accelerating voltage of 80 kV. CS suspension, with negative staining, was dropped onto copper grids coated with carbon support film for observation. Negative staining involved application of ~10 μL of 2% uranyl acetate solution to the grid. In all cases, excess liquid was blotted from the sample by lightly touching the edge of the grid with an edge or corner of filter paper. A Nikon (Tokyo, Japan) MDA502AA E400 polarized optical microscope (POM) was used for observation of LC film sandwiched between glass slides. Tensile properties of the chitosan films were measured using an Instron 5582 test-

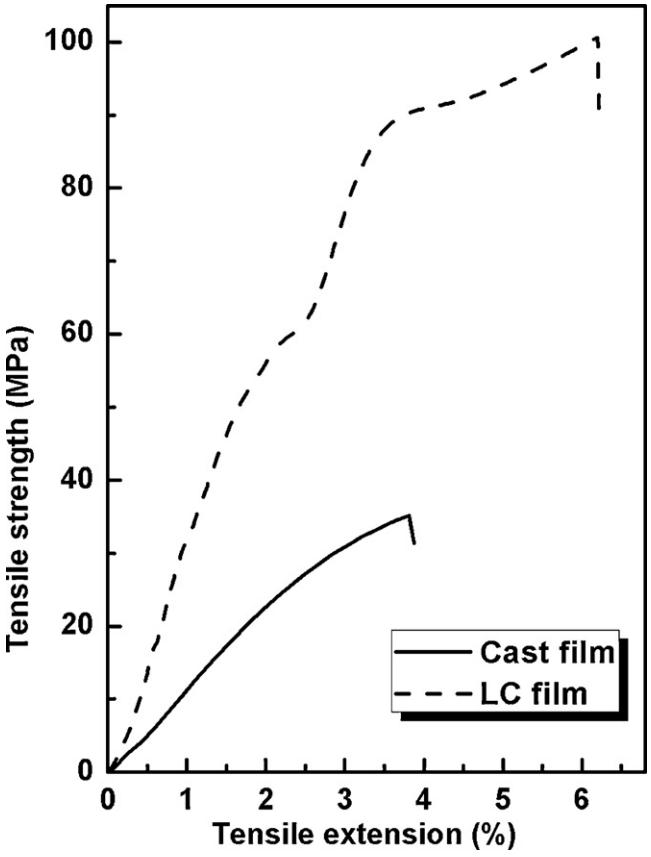

Fig. 2. Stress–strain curves of chitosan LC film and cast film.

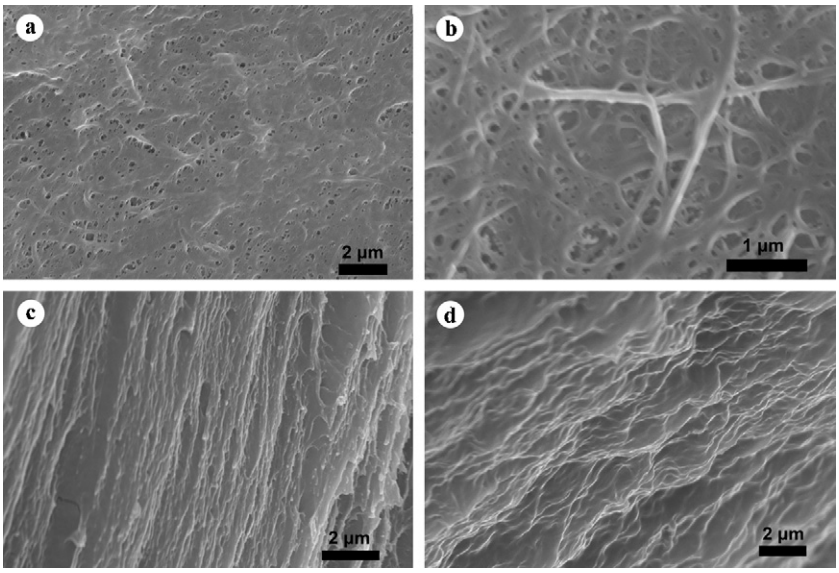

Fig. 3. SEM micrographs of chitosan cast film (a and b) and LC film (c and d).

ing machine (Instron Co., Norwood, MA) according to ASTM D882 standards. The testing speed for the film samples with dimensions of 0.1 mm × 10 mm × 40 mm was 10 mm/min. Five replicates were tested and the results averaged.

3. Results and discussion

Fig. 1 shows SEM (a) and TEM (b) images of chitosan nanofibers, and POM micrographs (c and d) of chitosan LC film. The combination of wet-grinding and high pressure homogenization resulted in the chitosan bulk being defibrillated into small bundles of nanofibrils, which were uniform nanofibers with an average diameter of 50 nm and a length of longer than 1 μm, as shown in Fig. 1(a). In contrast to the electrospun chitosan nanofibers, these disassembled nanofibrils had a smaller diameter (Geng, Kwon, & Jang, 2005). TEM of chitosan nanofibers, negatively stained with a 2% uranyl acetate solution, is shown in Fig. 1(b). It can be seen that the large sized fibers were split apart side-by-side by the strong mechanical forces. The nanofibers, with various widths, consisted of bundles of parallel fibrils of only about 1–5 nm in diameter. When viewed between the cross polarizers, the chitosan LC film showed ordered patterns with colors of sepia and blue from the POM micrographs in Fig. 1(c). The micro-scaled fingerprint exhibited in the sepia district indicated that the axes of the aligned chitosan LC were parallel to the preferred orientation. Fig. 1(d) shows that the texture was composed of curled arcs, somewhat like the cholesteric arrangements of chitin, collagen, or cellulose nanofibers discovered in biological tissues. There was no pattern or fingerprint found in the casting film revealing the liquid crystalline property meaning that chitosan nanofibrils self-assembled into morphogenesis with cholesteric LC structure in LC film.

Stress–strain curves of the chitosan LC film and cast film are presented in Fig. 2. The chitosan cast film possessed a high tensile strength (about 35.8 ± 7.6 MPa) and Young's modulus (about 580.0 ± 21.8 MPa). However, the chitosan LC film had a stronger mechanical strength and Young's modulus, up to 100.5 ± 4.0 MPa, and 2.2 ± 0.2 GPa, respectively, a mechanical characteristic typical of LC polymers (Suto, Iwaya, Ohno, & Karasawa, 1991). From the two staged stress–strain curve of the LC film, the second stage was thought to be a reorientation of the ordered nanofiber. The self-organized LC film exhibited an obviously higher modulus and tensile strength than the cast film. Morphologies of the chitosan LC film and cast film investigated by SEM micrographs are shown in Fig. 3. The cast film exhibited a majority of nano-sized pores with diameters ranging from 50 to 500 nm as shown in Fig. 3(a) and (b). Larger pores varying in size from 0.5 to 1.0 μm were found on the surface of the films. Fig. 3(c) and (d) shows the cross-section and surface morphology of the LC film, respectively. Instead of a porous structure, a vein shaped surface and a multilayered cross-section were observed; hence, the nanofibrils were thought to be self-aligned along a vector director in nematic planes. And then these planes packed layer by layer with a continuous rotation to form a helical geometry resulting in the cholesteric LC observed in the POM micrographs. Based on the microstructure, it was inevitable to conclude that the mechanical strength and modulus of nanofibrous materials is correlated with the pore size and fiber alignment. Layer-by-layer structure with regular fiber orientation and free pores must be beneficial for improving yield stress and modulus of the film materials.

4. Conclusions

In summary, we demonstrated a method combining wet-grinding with high-pressure homogenization that was used to prepare chitosan nanofibers. Uniform nanofibers with an average diameter of 50 nm and a length of longer than 1 μm were fabricated without electrospinning. The chitosan nanofibrous film presented the characteristic cholesteric texture of LC after self-organization from colloidal suspension. It had a high tensile strength of 100.5 ± 4.0 MPa and a Young's modulus of 2.2 ± 0.2 GPa, which were attributed to the ordered, layered, and pore-free compact structure of the film. The innovative process described in this study for the production of chitosan nanofiber and nanofibrous LC film could open up a new frontier for biopolymeric nanofiber research.

Acknowledgements

This work is financially supported by Natural Science Foundation of China, and the United States Department of Agriculture CSREES grant.

References

Belamie, E., Mosser, G., Gobeaux, F., & Giraud-Guille, M. M. (2006). Possible transient liquid crystal phase during the laying out of connective tissues: Alpha-chitin and collagen as models. *Journal of Physics: Condensed Matter*, *18*, S115–129.

Bouligand, Y. (1978). Liquid crystalline order in biological materials. In A. Blumstein (Ed.), *Liquid crystalline order in polymers* (pp. 261–297). New York: Academic Press.

Bouligand, Y. (2008). Liquid crystals and biological morphogenesis: Ancient and new questions. *Comptes Rendus Chimie*, *11*, 281–296.

Geng, X. Y., Kwon, O. H., & Jang, J. H. (2005). Electrospinning of chitosan dissolved in concentrated acetic acid solution. *Biomaterials*, *26*, 5427–5432.

Gong, J., Hu, X. L., Wong, K. W., Zheng, Z., Yang, L., Lau, W. M., et al. (2008). Chitosan nanostructures with controllable morphology produced by a nonaqueous electrochemical approach. *Advanced Materials*, *20*, 2111–2115.

Jung, J. M., & Mezzenga, R. (2010). Liquid crystalline phase behavior of protein fibers in water: Experiments versus theory. *Langmuir*, *26*, 504–514.

Kato, T. (2002). Self-assembly of phase-segregated liquid crystal structures. *Science*, *295*, 2414–2418.

Lima, M. M. D., & Borsali, R. (2004). Rodlike cellulose microcrystals: Structure, properties, and applications. *Macromolecular Rapid Communications*, *25*, 771–787.

Roman, M., & Gray, D. G. (2005). Parabolic focal conics in self-assembled solid films of cellulose nanocrystals. *Langmuir*, *21*, 5555–5561.

Rout, D. K., Barman, S. P., Pulapura, S. K., & Gross, R. A. (1994). Cholesteric mesophases formed by the modified biological macromolecule 3,6-O-(butyl carbamate)-N-phthaloyl chitosan. *Macromolecules*, *27*, 2945–2950.

Suto, S., Iwaya, T., Ohno, Y., & Karasawa, M. (1991). Cellulosic solid films exhibiting cholesteric liquid crystalline order. 1. Tensile creep in vacuo for ethyl cellulose and hydroxypropyl cellulose. *Journal of Materials Science*, *26*, 3073–3080.

Vollrath, F., & Knight, D. P. (2001). Liquid crystalline spinning of spider silk. *Nature*, *410*, 541–548.